LAUNCH VEHICLE STIFFNESS BUDGET SENSITIVITY TO CONTROL STABILITY CONSTRAINTS

Patrizia Cotugno[(1)], Mirko Aveta[(1)], Alessandro Lopez[(1)], Giuseppe Leto[(1)], Gianluca Curti[(2)]

[(1)]*AVIO, patrizia.cotugno@avio.com*
[(1)]*AVIO, mirko.aveta@avio.com*
[(1)]*AVIO, alessandro.lopez@avio.com*
[(1)]*AVIO, giuseppe.leto@avio.com*
[(2)]*ESA-ESRIN, Gianluca.Curti@ext.esa.int*

ABSTRACT

In the design phase of a new launch vehicle, the stiffness budget analysis represents an essential task. Indeed, the stiffness of each item of the launch vehicle has a fundamental impact on the definition of the global bending modes' parameters and on the fulfilment of the launch vehicle stability requirements. This article focuses on a sensitivity analysis obtained by varying each structural item's stiffness and computing the launch vehicle worst-case stability margins.
A set of stiffness budget alternates has been considered and an Linear Fractional Representation (LFR) of the launch vehicle has been defined for each different design case. With this set-up, the structural stiffness needs have been verified with respect to the control related requirements and, for each case, a tuning of the bending filter has been performed using structured H_∞.
The proposed analysis allows to graphically assess which parameters mostly affect the fundamental bending modes' eigenfrequencies and shapes and to approximate the impact of stiffness budget changes in terms of launch vehicle performance in view of mass saving optimizations.
The VEGA-E (Evolution) launcher has been considered as a benchmark for the proposed design methodology.

1 INTRODUCTION

In the preliminary design of launch vehicles, the mass budget is of premium concern. Tsiolkovsky's equation shows that the more lightweight is the final mass after a boost, the higher are the expected performances. An important fraction of the final mass is provided by the launcher structure. The structural design needs to focus on several aspects, such as transportation, assembly, ground aerodynamic loads, lift-off loads, and various instabilities like coupled structure-propulsion instabilities or resonant burns in solid rocket motors. Additionally, transient engine dynamics, pyro shocks, as well as acoustic and thermal effects should also be taken into account. Ultimately, this leads to three major structural concerns:

1. *strength* and therefore the structure's resistance to a possible mechanical failure due to yielding under given load conditions
2. *structural stability* in order to prevent a structural item from a catastrophic collapse under load;
3. *stiffness* as it impacts the vehicle natural frequencies and global bending modes that can effect stability in flight.

However, it is common practice to not consider *stiffness* as a design driver for a multistage rocket[12][18]. A typical design process would be that described in Fig. 1. The design drivers are typically coming from *strength* since *structural stability* is usually less sizing. As outlined in [12], the process in Fig. 1 is usually "protected" by a requirement on the fundamental mode's eigenfrequency that is required to be sufficiently higher than the launcher rigid dynamics' bandwidth frequency during flight. This kind of analysis yields a controllability constraint, yet such a constraint can only be verified once the structural design is defined, since it is relevant to the computation of the global bending modes. Consequently, if important inconsistencies arise in terms of controllability, the impact on the masses may be such to justify a new design loop at system level. More likely, especially when a certain degree of know-how is applicable, design refinements or trade-off analyses can be carried out to optimize the launcher performance or correct losses of margins that could arise in the design iterations. The approach presented in this paper is intended to ease such work.

It has been questioned during VEGA-E's phase-B how the recent development of robust control methodologies [9][14] and advanced modelling tools such as linear fractional representations (LFRs) [6] could support the process described in Fig. 1 for what concerns the fulfillment of *stiffness* and stability requirements, possibly improving the performance of the launcher with a mass saving strategy. Indeed, LFRs and robust control methodologies have successfully been applied in co-design activities. In [5], it has been shown, by means of flight data, that LFRs robustly allow to predict the flutter envelope on the F-16A/B in Heavy Store configuration. In [11], a co-design of a large satellite flexible structure has been carried out by applying LFR modelling and designing a robust reduced order H_∞ controller to meet pointing and mass requirements. This work paved the way for the development of a specific Satellite Dynamics Toolbox for preliminary design phases [16].

As for launchers, a lot of research has been carried out in the past years in Europe [10]: [13] has shown how LFRs can be applied to carry out structured singular value analysis on the VEGA launch vehicle and [15] has proven the possibility to carry out structured-H_∞ tuning with an LFR of a launch vehicle.

Given these very promising results, an advanced design tool has been recently developed [19]. This tool also provides further insight and understanding of the underlying fundamental design trade-offs at system level, allowing a robust definition and justification of such system requirements. It includes also the definition of a formal approach for uncertainty quantification and modelling, blending together statistical interpretations, system-level margins and a control-theoretic understanding by using LFRs. By defining a generic multichannel design model, all high-level technical specifications for the control system are mathematically formalized, enabling robust optimization and worst case analysis. Specific practical difficulties for an effective industrialization, such as the need to smoothly schedule the control laws, controller discretization and the issue of dimensionality have been fully addressed with efficient workarounds.

In this paper, such tool has been used to compute a set of LFRs for various stiffness budget variants and *automatically* assess the impact on the launcher stability margins. In particular, this activity was aimed at finding stiffness *margins* on each item of the stiffness budget in terms of controllability, in order to provide immediate understanding of the impacts of design alternates arising from trade-off studies driven by other criteria.

The paper is organized as follows. In Section 2, a sensitivity analysis of the *stiffness* items has been performed to assess the impact of stiffness variations on the global bending modes (frequencies and shapes). In Section 3, each of such alternate of global bending modes has been processed in the robust control and modelling tool to assess the impact on the stability margins, allowing to provide specific constraints for each structural sub-part. Section 4 presents a general trade-off analysis showing the impact of a stiffness variation both in terms of stability margins and launcher performance improvement. Finally, conclusions are drawn in Section 5.

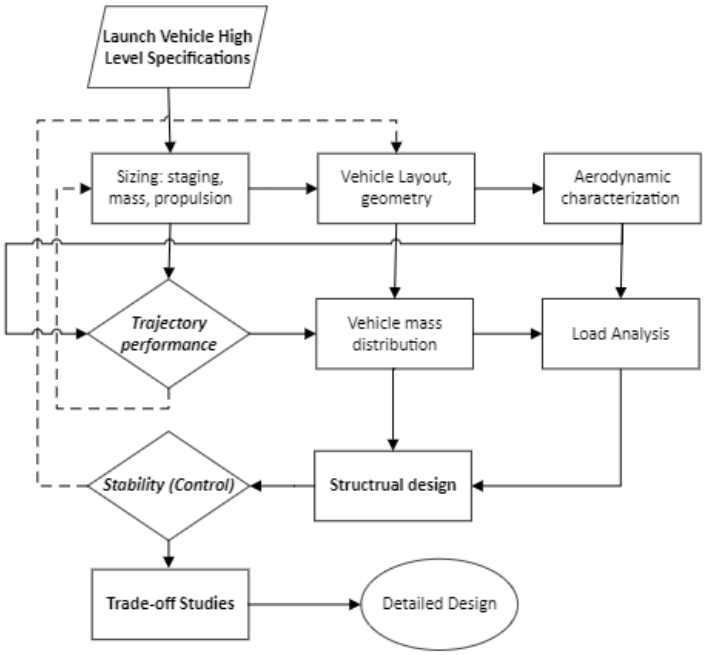

Figure 1: Typical System Design Cycle

2 BENDING MODES' SENSITIVITY TO STIFFNESS BUDGET

During the early phases of a launch vehicle development, when the structural properties are not yet well defined, it is of primary importance to have simplified models which allow to understand rapidly and efficiently how the launcher's global performance are affected by its driving parameters. Since a high fidelity 3D Finite Element Model (FEM) is not available in such phases, the bending modal properties can be assessed with a simplified 1D-beam Euler-Bernoulli theory. Indeed, since the launcher is a structure with an axial dimension significantly larger than the others, this theory represents a powerful tool for such preliminary assessments. The launch vehicle has been divided into several subsystems (e.g. stages and interstages) modelled as a series of 1D beams with known stiffness and mass properties, as illustrated in Fig. 2.

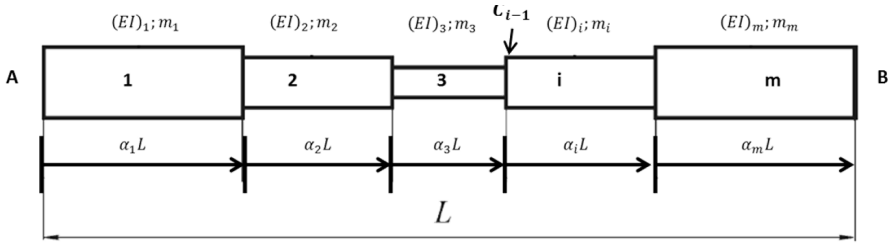

Figure 2: LV Simplified Model with 1D Beams

Thus, for each beam element, the Euler-Lagrange equation can be computed:

$$\frac{\partial^2}{\partial x^2}\left(EI\frac{\partial^2 v(x,t)}{\partial x^2}\right)+\rho A\frac{\partial^2 v(x,t)}{\partial t^2}=p_y(x,t) \tag{1}$$

where x represents the axial direction, $v\,(x,t)$ is the deformation along the y direction at time t and $p_y\,(x,t)$ is the vertical load per unit length.
Since bending mode analysis is carried out under free vibration conditions, $p_y\,(x,t)$ is null. Moreover, each sub-system (S/S) is assumed to have a constant stiffness EI, for the sake of simplicity.
The general solution of Eq.1 is of the kind: $v\,(x,t) = Re\,[Y\,(x)\,e^{-i\omega t}]$. Thus, by substituting the solution in Eq. 1, the following *spatial* problem can be analysed:

$$Y^{IV}(x)-\lambda Y(x)=0 \tag{2}$$

where $\lambda=\frac{\omega^2 EI}{\rho A}$. The general solution of Eq. 2 can be written as:

$$Y(x)=A\sinh(\lambda x)+B\cosh(\lambda x)+C\sin(\lambda x)+D\cos(\lambda x) \tag{3}$$

For a multi-beam body, the above equation shall consider the whole set of sub-structures. Therefore, if N_{ss} is the total number of beams, Eq. 4 holds:

$$Y(x)=\sum_{m=1}^{N_{ss}}\left(A_m\sinh(\lambda_m x_m)+B_m\cosh(\lambda_m x_m)+C_m\sin(\lambda_m x_m)+D_m\cos(\lambda_m x_m)\right) \tag{4}$$

with $4\times N_{ss}$ constants which can be evaluated by imposing the same number of boundary conditions (BCs). For the external boundary points, the following BCs can be written (free-free BCs):

- Null momentum: $E_m I_m Y_m^{II}(x_m)=0$ at $x_m=0$ and $x_m=L_{tot}$
- Null shear: $E_m I_m Y_m^{III}(x_m)=0$ at $x_m=0$ and $x_m=L_{tot}$

Whereas, for the internal boundary points:

- Continuity of displacement between two adjacent beams: $Y_m(x_m)=Y_{m+1}(0)$
- Continuity of rotation between two adjacent beams: $Y_m^I(x_m)=Y_{m+1}^I(0)$
- Balance of momentum between two adjacent beams: $E_m I_m Y_m^{II}(x_m)+E_{m+1}I_{m+1}Y_{m+1}^{II}(0)=0$
- Balance of shear between two adjacent beams: $E_m I_m Y_m^{III}(x_m)-E_{m+1}I_{m+1}Y_{m+1}^{III}(0)=0$

Solving the corresponding eigenvalue problem, the bending natural frequencies and shapes can be evaluated.
The above 1D theory is very suitable to perform a sensitivity analysis. At this purpose, starting from a nominal setting, the stiffness of each sub-system has been varied in the range [-20%,20%] with respect to its nominal value. Then, the properties which mostly impact the launcher's flexible behaviour, have been collected.
Fig. 3 shows, for example, how the S/Ss stiffness variations affect the first bending frequency. Similar figures can be obtained for the other modal parameters.
For the present study, the aforementioned modelling has been employed to conduct a sensitivity analysis of the modal parameters to the S/Ss stiffness variations. For this scope it is not needed to analyse the bending parameters for the whole trajectory. It is sufficient to analyse the worst case condition from a controllability point of view, given by the worst-case ratio between aerodynamic efficiency and thrust efficiency.

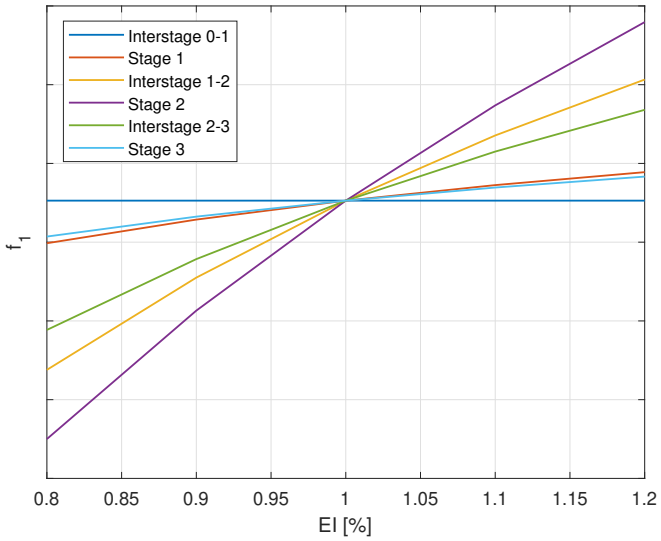

Figure 3: 1st Bending Frequency Sensitivity to S/S Stiffness Variation

3 ROBUSTNESS TO STIFFNESS BUDGET ALTERNATES

With the set-up described in the previous section, the structural stiffness needs have been verified with respect to the control related requirements by examining all the considered data sets from the stability point of view.

The task of stabilizing a launch vehicle is assigned to the Thrust Vector Control (TVC) system. A detailed description of the VEGA launcher's control law can be found in [7]. Its architecture is traditionally divided in two parts: the rigid-body controller, responsible for managing the rigid-body dynamics, and the bending filter, essential for the stabilization of the bending modes. The VEGA-E launcher has inherited this type of control architecture from its predecessors.

The main task of this control system is robust stabilization, since the launcher is made intrinsically unstable by the aerodynamic torque. At this purpose, high-level stability requirements have been defined.

Among these requirements, three specifications are imposed on the rigid-body dynamics: the Low Frequency Gain Margin (LFGM), the Low Frequency Delay Margin (LFDM), and the High Frequency Gain Margin (HFGM). Whereas, the remaining two specifications are applied to the flexible-body dynamics: the First Bending Mode Delay Margin and the Upper Bending Modes' Attenuation (BMU Att). All such high-level technical specifications are expressed as "stability margins", representing the distance from a critical point which signifies instability. As shown in Fig. 4, these specifications can be easily visualized on a Nichols Chart, which lends itself well to the verification of this type of requirements.

The stiffness of each item of the launch vehicle has an impact mainly on its flexible dynamics, and so on the definition of the bending modes' frequencies and shapes. At this purpose, for each case taken under study, a tuning of the bending filter has been performed in order to check if by varying the stiffness of a particular structural item it is still possible to satisfy the desired stability margins. The rigid body controller has instead been kept invariant as the rigid dynamics are scarcely influenced by stiffness variations, and also considering that a generic tuning of rigid gains and filters is already available in the framework of the VEGA E launcher.

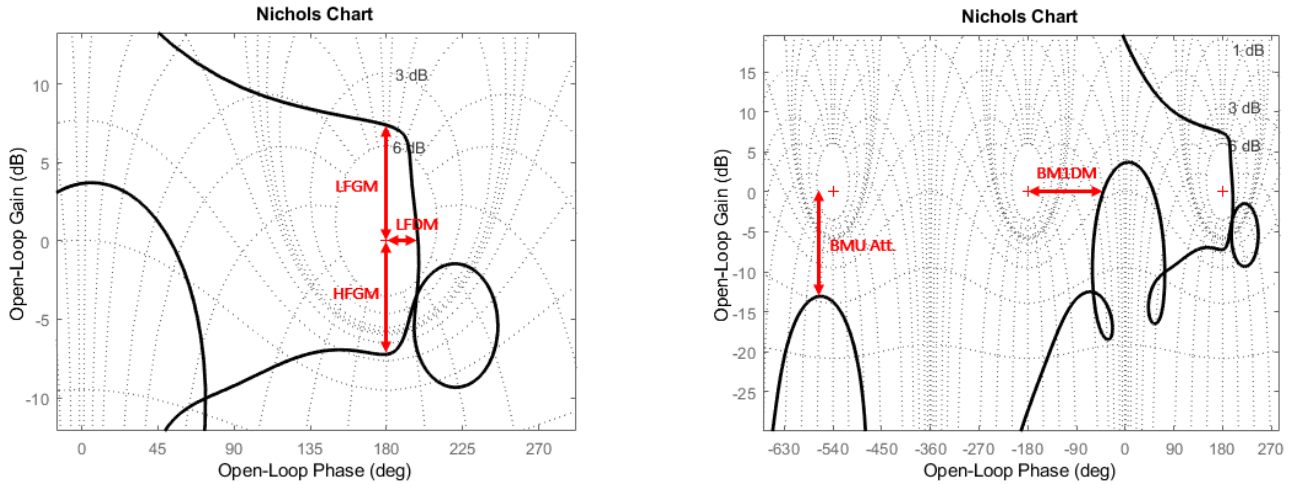

(a) Rigid-Body Margins

(b) Flexible-Body Margins

Figure 4: Stability Requirements

The challenge of controlling the flexible dynamics of a launch vehicle is given by the close proximity of the first bending mode frequency to the rigid-body control bandwidth. Indeed, the bending filter must be able to notch the bending modes without worsening the stability and performance goals achieved by the rigid-body controller. It is important to note that by decreasing the stiffness of each element, this task becomes more and more difficult as the first bending mode approaches the rigid body bandwidth. Moreover, the assignment of satisfying stability requirements needs to be extended beyond nominal conditions, encompassing all potential non-nominal scenarios, which include parametric uncertainties and disturbances. Hence, the use of a robust control techniques, including LFR modeling and structured H_∞ control [14], have been deemed appropriate, thanks to their demonstrated effectiveness in handling such uncertain systems.

3.1 LINEAR FRACTIONAL REPRESENTATION OF A LAUNCH VEHICLE

An LFR of the launch vehicle has been defined in order to explicitly include in the plant design all the system uncertainties and the information about how the launcher parameters are correlated to each other.
The process needed to obtain an LFR of a launch vehicle is summarized in the following steps [19]:

1. Collect and standardize the available data packages in order to define all the input scatterings either as percentage, range or plus-minus scatterings.

2. Perform a Monte-Carlo analysis in order to grasp uncertainties arising from trajectory dispersions.

3. Extract correlation between input scatterings and output parametric dispersions.

The primary objective of an LFR is precisely to establish the relationships between the input fundamental scatterings that affect the trajectory and the output parameters.
In order to determine the level of correlation between each output and its corresponding input scatterings, Pearson Correlation Coefficients (PCC) [2] have been computed for each parameter at constant Non-Gravitational Velocity (VNG), which is the controller's scheduling variable [7]. Then, by setting a threshold on the PCC values, the dominant correlations have been identified. A simple linear

regression model is used to represent such dependencies:

$$\hat{y} = y_0 + \frac{\overline{r} - \underline{r}}{2} + \sum_{i=1}^{n_i} \delta x_i \hat{\beta}_i + \frac{\overline{r} + \underline{r}}{2} \delta r_y \tag{5}$$

where two sets of uncertain parameters "enter" the Δ of the LFR: the "fundamental" scatterings δ_{xi} and the residual scatterings δ_{ry}.
As shown in Eq. 5, it is not recommended to disregard the residual scattering, as it may yield a significant impact, particularly when none of the fundamental input scatterings exert a dominant influence. Therefore, residuals whose H_∞ norm exceed a predefined threshold have been considered as independent scatterings. This approach for the design of LFRs appears always as a balance between two thresholds [19]: the threshold on the PCCs that quantify how many dependencies are to be modelled and the threshold on the residuals. By reducing the threshold on the PCCs, a greater number of dependencies are incorporated into the model, resulting in decreasing residuals and reduced conservatism. Similarly, by raising the threshold on the residuals the number of uncorrelated dispersions included in the model decreases, again reducing conservatism. Nevertheless, it is important to prevent the dimensions of the LFR from becoming excessively large. This can result in numerical errors and an excessive computational burden.
Each output parameter in Eq. 5 is finally constructed as a Redheffer star product of two systems: a completely nominal matrix and a completely uncertain matrix. By including all such parameters in the generalized state-space model, the launcher LFR is obtained as a Redheffer connection of a real diagonal uncertain matrix Δ and a nominal plant M.

3.2 BENDING FILTER TUNING

As explained in the previous sections, the stiffness of each subsystem has been systematically varied within the range [-20%,20%] and an uncertain LFR of the launch vehicle has been defined for each design case. All such cases have been examined from the stability point of view, by performing a tuning of the bending filter using structured H_∞.
The slosh masses, according to the reduced-body approach [17], are removed from the FEM. Thus, the bending parameters related to each stiffness alternate have been computed considering three different values of slosh masses (minimum, nominal and maximum) to take into account slosh modelling uncertainties. Nevertheless, due to the fact that the three sloshing cases essentially represent the same design scenario, a unique tuning of the bending filter has been performed to encompass the dispersed sloshing parameters.
The analyses have been repeated for two sizing payloads (PLs) and trajectories as the payload mass is another factor that adds variability to the bending modes.
The goal is to find the optimal tuning parameters that satisfy the specified stability requirements. Yet, to perform optimization it is needed to robustly formalize the design requirements into mathematical functions. Indeed, all high-level technical specifications are translated into constraint functions $\boldsymbol{g}$ or objective functions $\boldsymbol{f}$, all modelled as weighted H_∞ low-level requirements on appropriately selected channels of the generalized state space model. This dynamic programming problem can be seen as a sequence of two sub-problems of the form:

$$\min_x \max_\delta (\alpha \boldsymbol{f}(x, \delta), \boldsymbol{g}(x, \delta)) \tag{6}$$

where x is a given vector of tunable parameters in the control law, δ is a set of uncertain parameters in the design model, $\boldsymbol{f}$ is the worst case objective function norm and $\boldsymbol{g}$ is the worst case constraint function norm.

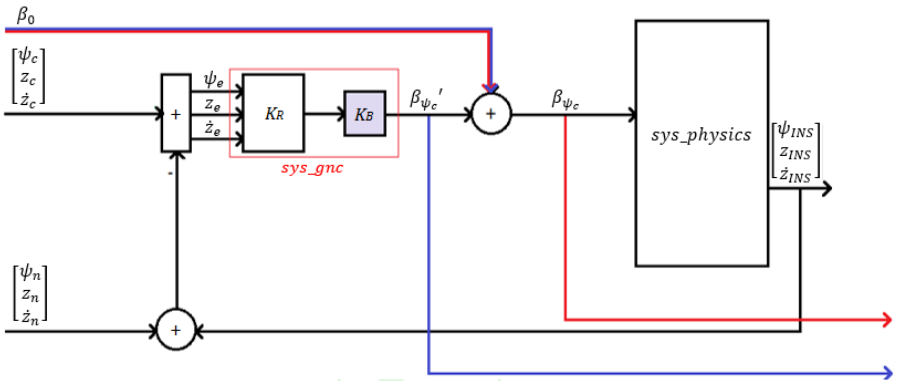

Figure 5: Closed-Loop System

Given its efficiency in the management of uncertain systems, SYSTUNE [14] has been identified as a suitable solver for this optimization problem. To accomplish this task, it dynamically adjusts the multiplier α until the solution of the subproblem converges to the solution of the original constrained optimization problem.
The subproblem,

$$\max_{\delta}(\boldsymbol{f}(\delta)) \tag{7}$$

is what we refer to as worst case (WC) analysis and is verified one requirement $f(\delta)$ at a time. At this purpose, the high level requirements in Fig. 4 are translated into H_∞ low level requirements over a given set of inputs and outputs of the closed-loop system model, illustrated in Fig. 5.
As can be noted, this multi-channel design model is composed of two main blocks:

- the controller *sys_gnc* which contains a non-tunable part, that is the rigid-body controller K_R and a tunable part, namely the bending filter K_B
- the plant *sys_physics* which contains the LFRs of the launch vehicle including the TVC subsystem.

The channels highlighted in red and blue are respectively the input sensitivity function S_i and the input complementary sensitivity function T_i. These two functions are essential for incorporating the stability requirements directly in the control design[1]. The translation from high-level requirements to low level requirements is summarized in Table 1 and makes use of the analytic link between the gain margin (GM) or phase margin (PM) and the H_∞ norm of the input sensitivity and complementary sensitivity functions, respectively $|S_{\beta_0 \to \beta_c}|_\infty$ and $|T_{\beta_0 \to \beta_c'}|_\infty$ [3]. However, the fact that the analytic link is explicit, should not suggest the reader that the low level requirements are exactly equal to the high level ones. The latter, in fact, being defined as purely gain or phase margins, do not need to be specified in a particular frequency range. Whereas, while verifying the low-level requirements, the WC norm may also be found at a frequency different than the crossover frequency of the stability margin. For this reason, as shown in Table 1, each metric is defined in a pertinent frequency range. This provides additional robustness as it allows to define a margin that contemplates mixed gain-phase perturbations.
Moreover, looking at Fig. 4, it should be noticed that the requirement on the upper bending modes is traditionally defined as an open loop requirement and not as a classical gain margin. Indeed, it is a requirement imposed on the magnitude of the open-loop function L. For this reason, it can be only translated in a low level requirement on the input complementary sensitivity function.

Table 1: Low Level Requirements

Metrics	**Low Level Requirements**		**Frequency Range**
LFGM	$\lvert S_{\beta_0 \to \beta_c} \rvert_\infty \leq \lvert \frac{GM}{GM-1} \rvert$	$\lvert T_{\beta_0 \to \beta_c'} \rvert_\infty \leq \lvert \frac{1}{GM-1} \rvert$	$f \leq \underline{f_{DM}}$
LFDM	$\lvert S_{\beta_0 \to \beta_c} \rvert_\infty \leq \lvert \frac{1}{2 \sin \frac{PM}{2}} \rvert$	$\lvert T_{\beta_0 \to \beta_c'} \rvert_\infty \leq \lvert \frac{1}{2 \sin \frac{PM}{2}} \rvert$	$\underline{f_{DM}} < f \leq \overline{f_{DM}}$
HFGM	$\lvert S_{\beta_0 \to \beta_c} \rvert_\infty \leq \lvert \frac{GM}{GM-1} \rvert$	$\lvert T_{\beta_0 \to \beta_c'} \rvert_\infty \leq \lvert \frac{1}{GM-1} \rvert$	$\overline{f_{DM}} < f \leq \overline{f_{HF}}$
BM1DM	$\lvert S_{\beta_0 \to \beta_c} \rvert_\infty \leq \lvert \frac{1}{2 \sin \frac{PM}{2}} \rvert$	$\lvert T_{\beta_0 \to \beta_c'} \rvert_\infty \leq \lvert \frac{1}{2 \sin \frac{PM}{2}} \rvert$	$\overline{f_{HF}} < f \leq \overline{f_{BM1}}$
BMU Att.	$\lvert T_{\beta_0 \to \beta_c'} \rvert_\infty \leq \lvert \frac{L}{1+L} \rvert$		$\overline{f_{BM1}} < f \leq f_{Nyquist}$

Regarding the tuning process, the bending filter has been parameterized in order to have a fixed structure. Thus, the control problem falls within the realm of the structured H_∞ techniques [8]. This approach enables us to overcome the limitations associated with the traditional unstructured H_∞, which often yield a full-order controller that is challenging to comprehend and implement within a specific practical control architecture. Moreover, traditional unstructured H_∞ may return solutions that prove to be fragile [4] when interpolating the control law against the scheduling variable.
The structure of the tunable bending filter is presented in Eq 8. It has been factorized into multiple second-order notch filters. Each cell has been parameterized using two variables: η_A and η_B, which determine the notch filter width and attenuation at the central frequency. The numerator and denominator frequencies have been selected to center each 2nd order filter around the expected dispersed modal frequencies. Actually, the filters' frequencies have been set as not tunable. This choice is done essentially to simplify the optimization problem. If a more complete tuning will be carried out, in any case, some considerations on structural stability need to be taken into account in order to avoid problems related to polynomial degeneracy. For the same reason, the free parameters have been constrained to vary in a limited range.

$$K_B(s) = \prod_{i=1}^{N} \frac{\frac{s^2}{\omega_{Ai}^2} + 2\frac{\eta_{Ai}}{\omega_{Ai}} s + 1}{\frac{s^2}{\omega_{Bi}^2} + 2\frac{\eta_{Bi}}{\omega_{Bi}} s + 1} \tag{8}$$

Fig. 6 illustrates the shape of the tunable bending filter and how it can vary modifying its tunable parameters. During the optimization, the solver converts each tuning goal into a normalized scalar value and adjusts the tunable parameters to minimize the H_∞ norms related to the requirements defined in Table 1. Each requirement is intended to be fulfilled if the related norm is less than 1.

4 STABILITY AND PERFORMANCE SENSITIVITY TO STIFFNESS BUDGET

An extensive analysis has been carried out to assess the stability of the launch vehicle in a broad spectrum of scenarios. The stiffness of each component was considered at its minimum, nominal, and maximum value for both the examined PL configurations. Remarkably, all the analyzed cases have given satisfactory results from the stability point of view. Indeed, for each case it has been possible to identify a suitable tuning configuration able to meet the imposed stability requirements.
Normalized results, which provide a standardized representation of the data, have been documented in Figs. 7 and 8. These spider plots illustrate the stability and performance metrics in a comprehensive and visually informative manner, enabling a detailed analysis of the obtained outcomes. Although the sensitivity analysis has been conducted on all main components of the launcher (Interstage 0-1, Stage 1, Interstage 1-2, Stage 2, Interstage 2-3, Stage 3), for the sake of brevity, only the figures related to the

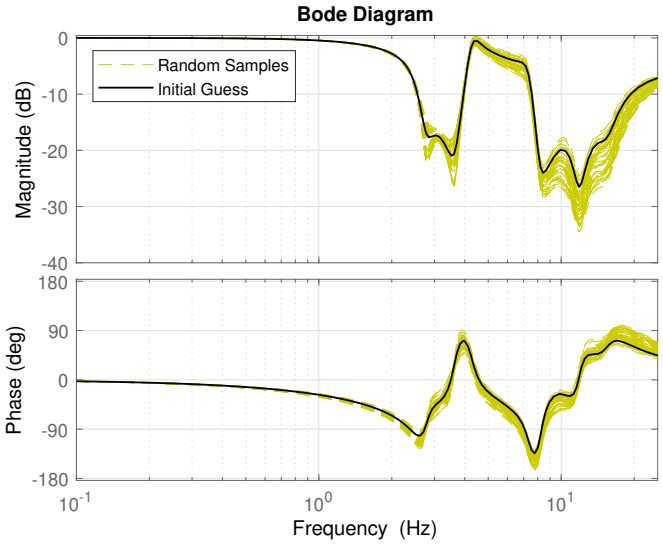

Figure 6: Tunable Bending Filter

upper components, specifically the Interstage 2-3 and the third stage, are here reported. This selection was made considering that the configuration of these two elements is currently in the design phase. On the contrary, the remaining components are inherited from previous launcher (VEGA-C) and their redesign is not being considered at present. However, for the purpose of comprehensive analysis, similar figures have been generated for all other subsystems, yielding analogous conclusions.

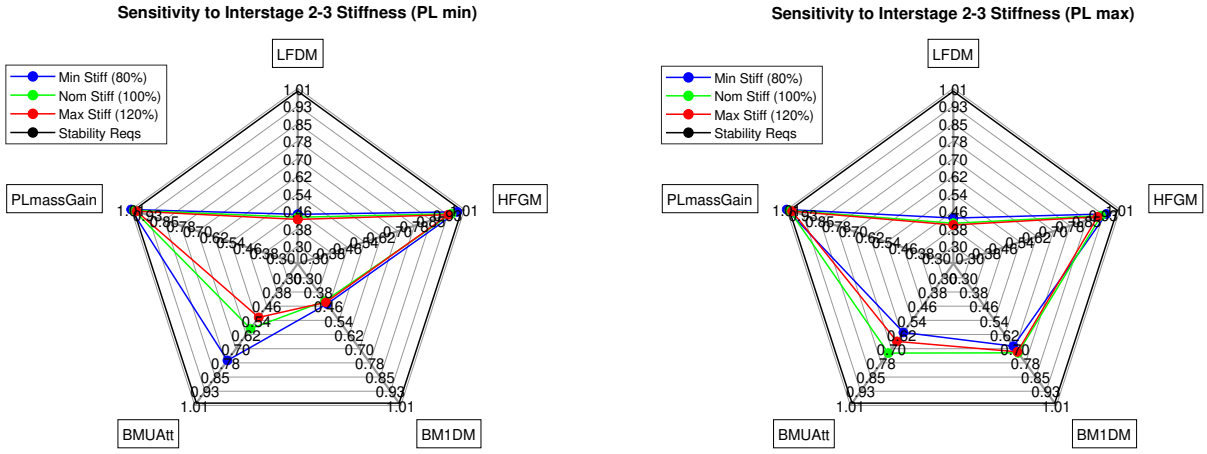

Figure 7: Sensitivity to Interstage 2-3 Stiffness Variations

It is worth noting from Figs. 7 and 8 that, as expected, as the stiffness of the subsystems decreases, the tuning of the bending filter becomes increasingly challenging, leading to reduced stability margins. To simplify the understanding of these plots, the norm related to the LFGM has been omitted since it cannot be influenced in any way by the tuning of the bending filter, which in fact does not act at very low frequencies. By examining these plots, immediate considerations can be made. Firstly, it can be noted that the High Frequency Gain Margin is the most penalized one as the norm associated to this requirement is close to 1. This outcome can be mainly attributed to the proximity of the first bending mode to the rigid-body bandwidth. Moreover, the reduction in stiffness has a relatively

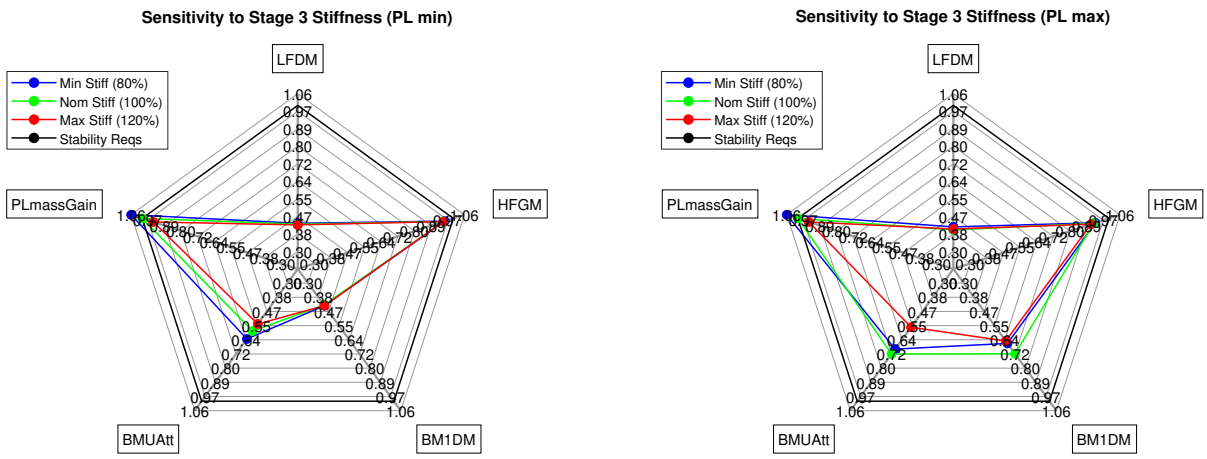

Figure 8: Sensitivity to Stage 3 Stiffness Variations

small impact on the rigid margins. In fact, the norms indicating the compliance with these requirements only exhibit slight variations among the cases of minimum, nominal, and maximum stiffness. However, reasonably it can be noted that as the stiffness decreases, the norm on these requirements increases, indicating a reduction of the stability margins due to the progressive lowering the first modal frequency. On the contrary, the stiffness variations predominantly influence the margins related to the flexible-body dynamics, such as the First Bending Mode Delay Margin and especially the Upper Bending Modes Attenuation. On these specifications, however, the margin is large enough to allow the solver to always find a good trade-off and ensure the fulfilment of all requirements.
In addition to assessing the structural stiffness variations with respect to control stability requirements, their impact on the launch vehicle performance has been examined. Notably, one of the vertices of the spider plots represents a norm related to the PL mass variation corresponding to each stiffness case. This norm serves as an indicator of the predicted delta performance, which is calculated using the performance derivatives. This delta is determined by assuming a linear correlation between stiffness variation and structural mass variation. Consequently, the minimum stiffness always corresponds to the maximum PL mass gain, although the specific ratio is determined by the linear correlation.

5 CONCLUSIONS

In conclusion, this article discusses how stiffness acts as a design driver for launch vehicles, along with strength and structural stability. In the design phase of a new launch vehicle, in fact, the mass budget is crucial, and the structural design plays a significant role in determining the final mass and the expected performance.
Traditionally, stiffness has not been considered a design driver for multistage rockets. However, recent developments in robust control methodologies and advanced modeling tools, such as Linear Fractional Representations (LFRs), enable new opportunities to improve the design process and optimize launcher performance while ensuring the fulfillment of stability requirements.
The article presents an advanced design methodology that makes use of LFRs and robust control techniques to assess the impact of stiffness variations on launcher stability margins.
The analyses carried out in this context are thoroughly described, encompassing the sensitivity analysis of stiffness variations on the global bending modes, the process of obtaining an LFR of the launch vehicle and the methodology used for the bending filter tuning. Finally a trade-off analysis of stiffness variations in terms of stability margins and launcher performance improvement is presented.

This kind of analysis enables the possibility to carry out mass-saving activities and structural optimization knowing the limitations given by the control system. Moreover, it allows to assess the impact of stiffness variations that are driven by other design drivers, providing useful insight to the system engineering of a launch vehicle.
In summary, results highlight that, within the range of explored stiffness variations, the required stability margins are consistently guaranteed. Additionally, certain examined cases show potential for increasing the performance of the launch vehicle, provided that the other structural design concerns are fulfilled (i.e.: load analysis).

6 ACKNOWLEDGEMENTS

We are deeply grateful to Samir Bennani and Pedro Simplicio for their important support in the design and follow-up of the advanced design tool [19] in the frame of esa contract no.4000124574/18/nl/crs.

REFERENCES

[1] M. G. Safonov, A. J. Laub, and G. Hartmann, "Feedback properties of multivariable systems: The role and use of the return difference matrix," *IEEE Transactions on Automatic Control*, vol. 26, 1981.

[2] J. Rodgers and A. Nicewander, "Thirteen ways to look at the correlation coefficient," *American Statistician - AMER STATIST*, vol. 42, pp. 59–66, Feb. 1988.

[3] K. Zhou and J. C. Doyle, *Essentials of Robust Control*. Prentice-Hall, 1998.

[4] D. Afolabi, *Catastrophes in Control Systems*. Darsaki Publications, 2002.

[5] S. Bennani, B. Beuker, J. W. Van Staveren, and J. J. Meijer, "Flutter analysis of an f-16a/b in heavy store configuration," *Journal of aircraft*, vol. 42, no. 6, pp. 1565–1574, 2005.

[6] S. Hecker, A. Varga, and J.-F. Magni, "Enhanced lfr-toolbox for matlab," *Aerospace Science and Technology*, vol. 9, no. 2, pp. 173–180, 2005.

[7] C. Roux and I. Cruciani, "Scheduling schemes and control law robustness in atmospheric flight of vega launcher," in *Proceedings of the 7th ESA International Conference on Spacecraft Guidance, Navigation and Control Systems*, 2008, pp. 1–5.

[8] P. Apkarian, P. Gahinet, and C. Buhr, "Multi-model, multi-objective tuning of fixed-structure controllers," *2014 European Control Conference (ECC)*, 2014.

[9] E. Chambon, P. Apkarian, and L. Burlion, "Flexible launch vehicle control using robust observer-based controller obtained through structured h synthesis," in *Advances in Aerospace Guidance, Navigation and Control: Selected Papers of the Third CEAS Specialist Conference on Guidance, Navigation and Control held in Toulouse*, Springer, 2015, pp. 23–38.

[10] A. Marcos, S. Bennani, C. Roux, and M. Valli, "Lpv modeling and lft uncertainty identification for robust analysis: Application to the vega launcher during atmospheric phase," *IFAC-PapersOnLine*, vol. 48, no. 26, pp. 115–120, 2015.

[11] H. H. S. Murali, D. Alazard, L. Massotti, F. Ankersen, and C. Toglia, "Mechanical-attitude controller co-design of large flexible space structures," in *Advances in Aerospace Guidance, Navigation and Control: Selected Papers of the Third CEAS Specialist Conference on Guidance, Navigation and Control held in Toulouse*, Springer, 2015, pp. 659–678.

[12] B. Suresh and K. Sivan, *Integrated design for space transportation system*. Springer, 2015.

[13] P. Simplıcio, S. Bennani, A. Marcos, C. Roux, and X. Lefort, "Structured singular-value analysis of the vega launcher in atmospheric flight," *Journal of Guidance, Control, and Dynamics*, vol. 39, no. 6, pp. 1342–1355, 2016.

[14] P. Apkarian and D. Noll, "The H∞ Control Problem is Solved," *Aerospace Lab*, no. 13, pages 1–11, Nov. 2017.

[15] D. Navarro-Tapia, A. Marcos, P. Simplicio, S. Bennani, and C. Roux, "Legacy recovery and robust augmentation structured design for the vega launcher," *International Journal of Robust and Nonlinear Control*, vol. 29, no. 11, pp. 3363–3388, 2019.

[16] D. Alazard and F. Sanfedino, "Satellite dynamics toolbox for preliminary design phase," in *43rd Annual AAS Guidance and Control Conference*, vol. 30, 2020, pp. 1461–1472.

[17] T. M. Barrows and J. S. Orr, *Dynamics and Simulation of Flexible Rockets*. Academic Press, 2020.

[18] D. Edberg and W. Costa, *Design of Rockets and Space Launch Vehicles*. American Institute of Aeronautics and Astronautics, Inc., 2020.

[19] M. Aveta, "Adaptive flight guidance and control systems with reconfiguration, [final report], esa contract no.4000124574/18/nl/crs," 2023.